Journal of Sound and Vibration (1999) **222**(2), 259–279
Article No. jsvi.1998.2078, available online at http://www.idealibrary.com on IDEAL

MODAL ANALYSIS OF SERPENTINE BELT DRIVE SYSTEMS

L. ZHANG AND J. W. ZU

Department of Mechanical and Industrial Engineering, University of Toronto, 5 King's College Road, Toronto, Ontario, Canada, M5S 3G8

(*Received* 27 *July* 1998, *and in final form* 19 *October* 1998)

The modal analysis of linear prototypical serpentine belt drive systems is performed in this study. The entire system is divided into two subsystems: one with a single belt and its motion is not coupled to the rest of the system in the linear analysis; the other with the remaining components. The explicit exact characteristic equation for eigenvalues is derived, which does not use the iteration approach. This characteristic equation can provide insight concerning the effect of design parameters on natural frequencies of the system. The response of serpentine belt drive systems to arbitrary excitations is obtained as a superposition of orthogonal eigenfunctions. The exact solution without using eigenfunction expansion is derived when the excitations are non-resonance harmonic. This explicit expression is particularly useful in the direct perturbation analysis of the corresponding non-linear problems.

1. INTRODUCTION

The dynamic analysis of the whole serpentine belt drive system is a challenging subject and it has been investigated for only 15 years. Two distinct types of system vibrations exist in belt drive systems: (1) transverse vibrations in various belt spans and (2) rotational vibrations of pulleys with the belt spans serving as coupling springs.

Transverse vibrations of belt spans are an example of an axially moving material which has been investigated extensively. For linear vibration analysis, Skutch [1] first determined the natural frequencies of a moving string by superposition of two waves propagating in opposite directions. Archibald and Emslie [2] considered the same problem but derived the equations using a variational approach. The classical modal analysis, which is applied to the linear non-translating string model, is not directly applicable to linear axially moving strings since the generalized co-ordinates in an eigenfunction expansion remain coupled. Wickert and Mote [3] modified the classical modal analysis method by casting the equations of motion for a travelling string into a canonical, first order form that is defined by one symmetric and one skew-symmetric matrix differential operator. When the equations of motion are represented in this form, the eigenfunctions are orthogonal with respect to each other. The response of

0022–460X/99/170259 + 21 $30.00/0

axially moving materials to arbitrary excitation and initial conditions can be represented in closed-form. The earliest calculation on the fundamental period of autonomous non-linear transverse vibrations of an axially moving tensioned string was given by Mote [4]. In the work done by Thurman and Mote [5], a hybrid discretization and perturbation method were employed to quantify the speed dependence of the deviation between the linear and non-linear fundamental periods for a broad range of amplitude and speed parameters. Bapat and Srinivasan [6] used the method of harmonic balance to obtain approximate results. More recently, Moon and Wickert [7] developed a modal perturbation solution in the context of the asymptotic method of Krylov, Bogoliubov and Mitropolsky for a continuous, non-autonomous and gyroscopic system with geometric non-linearity.

The rotational vibrations of serpentine drive systems have been studied in recent research. Hawker [8] investigated natural frequencies of damped drive systems with a dynamic tensioner. This study, however, does not consider the effect of the tensioner on either the equilibrium state or the dynamics response. Barker *et al.* [9] used a Runge–Kutta method to solve a rapid acceleration–deceleration case involving a movable Coulomb-damped tensioner arm. Hwang *et al.* [10] proposed a general model for the rotational response of the entire serpentine belt drive and applied the results to predict the onset of belt slip. For linear viscous damping, Kraver *et al.* [11] developed a complex procedure to solve both underdamped and overdamped systems.

The above works assume that the rotational and transverse motions are uncoupled for linear systems. This is only an approximation for accessory drives containing a dynamic tensioner while it is true for fixed-center systems. Ulsoy *et al.* [12] considered the coupling between the transverse motion of the belt and that of the tensioner. This model captures a parametric instability mechanism capable of causing large lateral belt vibrations due to tension fluctuations. Beikmann *et al.* [13] developed a prototypical model (two pulleys with a tensioner) to examine this coupling mechanism which led to new conclusions regarding linear free vibrations. The natural frequencies and mode shapes of an operating serpentine belt drive system were determined using analytical and experimental methods. A two-level iteration based on Holzer's method is employed to tackle the eigenvalue problem. Beikmann *et al.* [14] demonstrated that finite belt stretching created a non-linear mechanism that may lead to strong coupling between the pulley/tensioner rotational vibration and transverse belt vibration. Using the eigensolutions obtained from linear analysis, the non-linear vibration model was discretized and the coupled vibration response was evaluated numerically.

In the present study, as a first step to tackle the non-linear vibration analysis of serpentine belt drive systems, modal analysis is performed for the response of linear serpentine belt drive systems. The eigenvalues and eigenfunctions of the linear prototypical system were calculated in reference [13] by employing the iteration approach. Instead of using the iteration method, an explicit characteristic equation for natural frequencies of the prototypical system is obtained, which provides insight concerning the effects of design parameters on eigenvalues. The exact closed-form expressions for the dynamic response of the system subjected to arbitrary excitations and initial conditions are given using the eigenfunction expansion. Furthermore, for the steady state response of the system subjected to harmonic excitation, explicit exact expressions for the dynamic response are derived directly. These expressions will be used in the direct perturbation analysis of non-linear systems.

2. CANONICAL FORM OF THE EQUATIONS OF MOTION

Figure 1 defines the prototypical model which Beikmann *et al.* [13] developed. This model contains all the essential components present in automotive serpentine drives: (1) a driving pulley, (2) a driven pulley, (3) a dynamic tensioner and (4) a belt span fixed transversely at both ends. Several assumptions are made to simplify the modelling of the serpentine drive system: (1) damping is negligible, (2) belt bending stiffness is negligible, (3) axial translation speed of the belt, c, is constant and uniform, and (4) belt slippage is negligible.

Hamilton's Principle [13] is applied to derive the governing equations of motion and boundary conditions. The linear equations of motion for the belt spans are

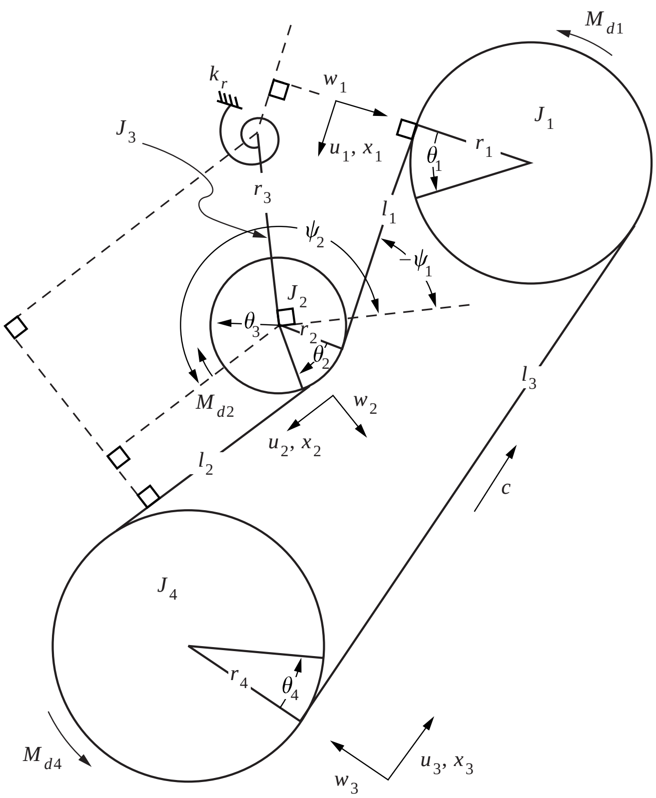

Figure 1. A prototypical three-pulley serpentine belt drive system.

$$m(w_{1,tt} + 2cw_{1,xt}) - P_{t1}w_{1,xx} = f_1(x, t), \tag{1}$$

$$m(w_{2,tt} + 2cw_{2,xt}) - P_{t2}w_{2,xx} = f_2(x, t), \tag{2}$$

$$m(w_{3,tt} + 2cw_{3,xt}) - P_{t3}w_{3,xx} = F_3(x, t), \tag{3}$$

with boundary conditions

$$w_1(0, t) = 0, \quad w_1(l_1, t) = \chi_3(t)\sin\psi_1, \tag{4}$$

$$w_2(0, t) = \chi_3(t)\sin\psi_2, \quad w_2(l_2, t) = 0, \tag{5}$$

$$w_3(0, t) = 0, \quad w_3(l_3, t) = 0, \tag{6}$$

where w_i is the transverse deflection in span i from equilibrium, m is the belt mass per unit, P_{ti} is the span tractive tension component in span i at equilibrium ($P_{ti} = P_{oi} - mc^2$, where P_{oi} is the total operating tension in span i), $f_1(x, t)$, $f_2(x, t)$ and $F_3(x, t)$ are the external excitations, l_i is the length of span i, $\chi_3(t)$ is the displacement of the tensioner arm along the arc-length, ψ_1 and ψ_2 are the alignment angles between the tensioner arm motion and the adjacent belt spans at equilibrium, and subscripts $,x$ and $,t$ denote the partial derivative with respect to x and t, respectively.

The linear equations of motion for the pulleys are

$$P_{d1} - P_{d3} + f_3(t) = m_1\ddot{\chi}_1, \quad P_{d2} - P_{d1} + f_4(t) = m_2\ddot{\chi}_2, \quad P_{d3} - P_{d2} + f_6(t) = m_4\ddot{\chi}_4, \tag{7 – 9}$$

where $\chi_i = r_i\theta_i$, $m_i = J_i/r_i^2$, and P_{di} are dynamic tensions in each span, induced by infinitesimal pulley and tensioner arm rotations:

$$P_{d1} = k_1(\chi_3\cos\psi_1 + \chi_2 - \chi_1), \quad P_{d2} = k_2(\chi_3\cos\psi_2 + \chi_4 - \chi_2), \quad P_{d3} = k_3(\chi_1 - \chi_4), \tag{10 – 12}$$

in which $k_i = EA/l_i (i = 1, 2, 3)$, E is the Young's modulus, and A is the cross-sectional area of the belt. The linearized equation of motion for the tensioner arm is

$$\begin{aligned}(-P_{t1}w_{1,x}(l_1, t) + mcw_{1,t}(l_1, t))\sin\psi_1 + (P_{t2}w_{2,x}(0, t) - mcw_{2,t}(0, t))\sin\psi_2 \\ - k_1(\chi_3\cos\psi_1 + \chi_2 - \chi_1)\cos\psi_1 - k_2(\chi_3\cos\psi_2 + \chi_4 - \chi_2)\cos\psi_2 \\ - (k_s + k_{gr})\chi_3 + f_5(t) = m_3\ddot{\chi}_3,\end{aligned} \tag{13}$$

where $k_s = k_r/r_3^2$, k_r is the rotational stiffness of the tensioner spring, and k_{gr} is the geometric tensioner stiffness defined as

$$k_{gr} = \frac{P_{t1}\sin\psi_1 - P_{t2}\sin\psi_2}{r_3}, \tag{14}$$

which is derived from the change of the tensioner arm displacement. Equation

(13) couples the tensioner arm motion to the transverse motion of the adjacent belt spans.

The modal analysis of the serpentine belt drive systems is applied to the linear equations of motion for the four discrete elements (three pulleys and one tensioner arm) and three continuous elements (the belt spans). It can be seen from equations (1)–(13) that for linear analysis, the transverse vibration of span 3 and vibration of other components are decoupled. Thus, it is desirable to divide the entire system into two subsystems: subsystem 1 which includes span 3 only and subsystem 2 which includes all the other parts of the system.

For subsystem 1, the equation of motion can be rewritten in operator form,

$$M_3\ddot{w}_3 + G_3\dot{w}_3 + K_3 w_3 = F_3, \tag{15}$$

where

$$M_3 = m, \quad G_3 = 2mc\frac{\partial}{\partial x}, \quad K_3 = -P_{t3}\frac{\partial^2}{\partial x^2}. \tag{16}$$

For subsystem 2, the equations of motion can be rewritten in matrix operator form,

$$\mathbf{M}\ddot{\mathbf{W}} + \mathbf{G}\dot{\mathbf{W}} + \mathbf{K}\mathbf{W} = \mathbf{F}, \tag{17}$$

where

$$\mathbf{F} = \{f_1(x,t) f_2(x,t) f_3(x,t) f_4(x,t) f_5(x,t) f_6(x,t)\}^T \tag{18}$$

and the displacement vector $\mathbf{W}$ is composed of the displacement of belt span 1, belt span 2, three pulleys and the tensioner arm

$$\mathbf{W} = \{w_1(x,t) w_2(x,t) \chi_1(t) \chi_3(t) \chi_3(t) \chi_4(t)\}^T. \tag{19}$$

The mass matrix operator $\mathbf{M}$, gyroscopic matrix operator $\mathbf{G}$, and stiffness matrix operator $\mathbf{K}$ are defined, respectively, as

$$\mathbf{M} = \begin{bmatrix} m & 0 & 0 & 0 & 0 & 0 \\ 0 & m & 0 & 0 & 0 & 0 \\ 0 & 0 & m_1 & 0 & 0 & 0 \\ 0 & 0 & 0 & m_2 & 0 & 0 \\ 0 & 0 & 0 & 0 & m_3 & 0 \\ 0 & 0 & 0 & 0 & 0 & m_4 \end{bmatrix}, \tag{20}$$

$$\mathbf{G} = \begin{bmatrix} 2mc\frac{\partial}{\partial x} & 0 & 0 & 0 & 0 & 0 \\ 0 & 2mc\frac{\partial}{\partial x} & 0 & 0 & 0 & 0 \\ 0 & 0 & 0 & 0 & 0 & 0 \\ 0 & 0 & 0 & 0 & 0 & 0 \\ -mc\sin\psi_1|_{l_1} & mc\sin\psi_2|_0 & 0 & 0 & 0 & 0 \\ 0 & 0 & 0 & 0 & 0 & 0 \end{bmatrix}, \tag{21}$$

$$\mathbf{K} = \begin{bmatrix} -P_{t1}\dfrac{\partial^2}{\partial x^2} & 0 & 0 & 0 & 0 & 0 \\ 0 & -P_{t2}\dfrac{\partial^2}{\partial x^2} & 0 & 0 & 0 & 0 \\ 0 & 0 & k_1+k_3 & -k_1 & -k_1\cos\psi_1 & -k_3 \\ 0 & 0 & -k_1 & k_1+k_2 & \begin{matrix} k_1\cos\psi_1 - \\ k_2\cos\psi_2 \end{matrix} & -k_2 \\ P_{t1}\sin\psi_1\dfrac{\partial}{\partial x}\Big|_{l_1} & -P_{t2}\sin\psi_2\dfrac{\partial}{\partial x}\Big|_0 & -k_1\cos\psi_1 & \begin{matrix} k_1\cos\psi_1 - \\ k_2\cos\psi_2 \end{matrix} & \begin{matrix} k_1\cos^2\psi_1 + \\ k_2\cos^2\psi_2 + k_4 \end{matrix} & k_2\cos\psi_2 \\ 0 & 0 & -k_3 & -k_2 & k_2\cos\psi_2 & k_2+k_3 \end{bmatrix}. \tag{22}$$

The presence of boundary terms in **G** and **K** appears to break skew or symmetry. It should be emphasized that taking the inner product $\langle \mathbf{W}, \mathbf{KW} \rangle$ involves integration terms by parts, which cancels with the non-zero boundary terms in **G** and **K**. Therefore, the serpentine belt drive system operating at non-zero axial belt speed constitutes a conservative gyroscopic system. The modal analysis of discrete gyroscopic systems was studied extensively [15, 16]. A similar study of a single axially moving span was conducted by Wickert and Mote [3] and their analysis can be applied directly to subsystem 1. Thus, the modal analysis of subsystem 1 will no longer be discussed in this paper. Instead, the focus of the present study will be on subsystem 2. Since the serpentine belt drive system is a hybrid system consisting of both discrete and continuous elements, a combination of both Meirovitch's and Wickert's methods suggested by Beikmann [13] is employed to formulate the eigenvalue problem and to evaluate the properties of the eigensolutions.

To apply the methods of Meirovitch [15] and Wickert and Mote [3] to the present continuous/discrete system, equation (17) should be cast in the first order form. Defining the state vector and the excitation vector

$$\mathbf{U} = \begin{Bmatrix} \dot{\mathbf{W}} \\ \mathbf{W} \end{Bmatrix}, \quad \mathbf{Q}(x, t) = \begin{Bmatrix} \mathbf{F}(x, t) \\ \mathbf{0} \end{Bmatrix}, \tag{23}$$

and matrix differential operators

$$\mathbf{A} = \begin{bmatrix} \mathbf{M} & \mathbf{0} \\ \mathbf{0} & \mathbf{K} \end{bmatrix}, \quad \mathbf{B} = \begin{bmatrix} \mathbf{G} & \mathbf{K} \\ -\mathbf{K} & \mathbf{0} \end{bmatrix}, \tag{24}$$

equation (17) becomes

$$\mathbf{A}\dot{\mathbf{U}} + \mathbf{B}\mathbf{U} = \mathbf{Q}. \tag{25}$$

Equation (25) is the canonical form of the equations of motion and its solution satisfies the appropriate boundary conditions and initial conditions.

The inner product of two vectors $\mathbf{U}_n$ and $\mathbf{U}_r$ is defined as

$$\langle \mathbf{U}_n, \mathbf{U}_r \rangle = \int_0^1 (\dot{w}_{1n}\bar{\dot{w}}_{1r} + w_{1n}\bar{w}_{1r})\,\mathrm{d}x + \int_0^2 (\dot{w}_{2n}\bar{\dot{w}}_{2r} + w_{2n}\bar{w}_{2r})\,\mathrm{d}x + \dot{\boldsymbol{\chi}}_n^T \bar{\dot{\boldsymbol{\chi}}}_r + \boldsymbol{\chi}_n^T \bar{\boldsymbol{\chi}}_r, \tag{26}$$

where the overbar denotes complex conjugation. With respect to this inner product, the operators $\mathbf{A}$ and $\mathbf{B}$ satisfy several properties which are the cornerstones of the subsequent analysis. First, operator $\mathbf{A}$ is symmetric, and $\mathbf{B}$ is skew symmetric; namely,

$$\langle \mathbf{AU}_n, \mathbf{U}_r \rangle = \langle \mathbf{U}_n, \mathbf{AU}_r \rangle, \quad \langle \mathbf{BU}_n, \mathbf{U}_r \rangle = -\langle \mathbf{U}_n, \mathbf{BU}_r \rangle. \tag{27}$$

Second, operator $\mathbf{A}$ is positive definite for sufficiently low transport speed. Dynamic systems described by one symmetric and one skew-symmetric operator are termed gyroscopic systems.

3. EIGENVALUES AND EIGENFUNCTIONS

The eigenvalue problem of subsystem 2 can be studied in the context of gyroscopic dynamic systems when the equation of motion is cast in operator form. The separable solution

$$\mathbf{U}(x, t) = \mathrm{Re}\{\boldsymbol{\Psi}_n\, \mathrm{e}^{\lambda_n t}\} \tag{28}$$

leads to the eigenvalue problem

$$\lambda_n \mathbf{A}\boldsymbol{\Psi}_n + \mathbf{B}\boldsymbol{\Psi}_n = \mathbf{0}, \tag{29}$$

where λ_n and $\boldsymbol{\Psi}_n$ are complex. The eigensolutions satisfy several properties [13]. The eigenvalues are imaginary; namely, $\lambda_n = i\omega_n$, where ω_n is the real oscillation frequency. Furthermore, the eigenfunctions $\boldsymbol{\Psi}_n$ have the structure

$$\boldsymbol{\Psi}_n = \boldsymbol{\Psi}_n^R + i\boldsymbol{\Psi}_n^I, \tag{30}$$

$$\boldsymbol{\Psi}_n^R = \begin{Bmatrix} -\omega_n \boldsymbol{\phi}_n^I(x) \\ \boldsymbol{\phi}_n^R \end{Bmatrix}, \quad \boldsymbol{\Psi}_n^I(x) = \begin{Bmatrix} \omega_n \boldsymbol{\phi}_n^R(x) \\ \boldsymbol{\phi}_n^I(x) \end{Bmatrix}. \tag{31}$$

Here, $\boldsymbol{\phi}_n(x)$ is the normalized eigenfunction associated with the displacement field which can be expressed as

$$\boldsymbol{\phi}_n(x) = \{\phi_{1n}(x)\phi_{2n}(x)\hat{\chi}_{1n}\hat{\chi}_{2n}\hat{\chi}_{3n}\hat{\chi}_{4n}\}^T, \tag{32}$$

where ϕ_{1n} and ϕ_{2n} are the normalized eigenfunctions of transverse displacements $w_1(x, t)$ and $w_2(x, t)$. $\hat{\chi}_{1n}$, $\hat{\chi}_{2n}$, $\hat{\chi}_{3n}$ and $\hat{\chi}_{4n}$ are normalized eigenfunctions associated with the displacement of discrete components. The eigenfunctions $\boldsymbol{\Psi}_n$ satisfy the orthonormality relations

$$\langle \mathbf{A}\boldsymbol{\psi}_n^R, \boldsymbol{\psi}_m^R \rangle = \delta_{nm}, \quad \langle \mathbf{A}\boldsymbol{\psi}_n^I, \boldsymbol{\psi}_m^I \rangle = \delta_{nm}, \quad \langle \mathbf{A}\boldsymbol{\psi}_n^R, \boldsymbol{\psi}_m^I \rangle = 0, \tag{33}$$

$$\langle \mathbf{B}\boldsymbol{\psi}_n^R, \boldsymbol{\psi}_m^R \rangle = 0, \quad \langle \mathbf{B}\boldsymbol{\psi}_n^I, \boldsymbol{\psi}_m^I \rangle = 0, \quad \langle \mathbf{B}\boldsymbol{\psi}_n^R, \boldsymbol{\psi}_m^I \rangle = \omega_n \delta_{nm}. \tag{34}$$

Since the serpentine belt drive system is a hybrid system (part continuous and part discrete), the usual approaches to solve the corresponding eigenvalue problem are not applicable. Beikmann *et al.* [13] used Holzer's method to solve the free vibration problems. Holzer's method involves two iteration loops: (1) an "inner loop" for the cyclic belt span/pulley, and (2) an "outer loop" for the tensioner arm. Iteration solutions were employed in both the inner loop and the outer loop and thus provide little indication of the effect of design parameters on natural frequencies. In the following study, instead of using the iteration solution, the direct solution method is used to derive the explicit exact characteristic equation.

It is assumed that the motion is harmonic, that is

$$\chi_i = \hat{\chi}_{in}\, \mathrm{e}^{i\omega t} (i = 1, 4), \quad w_i(x, t) = \phi_{in}(x)\, \mathrm{e}^{i\omega t}, (i = 1, 2). \tag{35}$$

Substituting equations (10)–(12) and (35) into equations (7)–(9), eliminating $\mathrm{e}^{i\omega t}$, and putting those terms including $\hat{\chi}_{3n}$ on the right of the equations yields

$$(k_1 + k_3 - m_1\omega^2)\hat{\chi}_{1n} - k_1\hat{\chi}_{2n} - k_3\hat{\chi}_{4n} = k_1 \cos\psi_1 \hat{\chi}_{3n}, \tag{36}$$

$$-k_1\hat{\chi}_{1n} + (k_1 + k_2 - m_2\omega^2)\hat{\chi}_{2n} - k_2\hat{\chi}_{4n} = (k_2 \cos\psi_2 - k_1 \cos\psi_1)\hat{\chi}_{3n}, \tag{37}$$

$$-k_3\hat{\chi}_{1n} - k_2\hat{\chi}_{2n} + (k_2 + k_3 - m_4\omega^2)\hat{\chi}_{4n} = -k_2 \cos\psi_2 \hat{\chi}_{3n}. \tag{38}$$

The sum of equations (36)–(38) leads to

$$m_1\hat{\chi}_{1n} + m_2\hat{\chi}_{2n} + m_4\hat{\chi}_{4n} = 0. \tag{39}$$

Inserting equation (39) into equations (36) and (38) and solving the resulting equations leads to

$$\hat{\chi}_{1n} = \frac{\left[\left(1 + \dfrac{m_4}{m_2}\right)k_2 + k_3 - m_4\omega^2\right]k_1 \cos\psi_1 + \left(\dfrac{m_4}{m_2}k_1 - k_3\right)k_2 \cos\psi_2}{\Delta}\hat{\chi}_{3n}, \tag{40}$$

$$\hat{\chi}_{2n} = \frac{\left(-\dfrac{m_1}{m_2}k_2 - \dfrac{m_1 + m_4}{m_2}k_3 + \dfrac{m_1 m_4}{m_2}\omega^2\right)k_1 \cos\psi_1}{\Delta}\hat{\chi}_{3n} + \frac{\left(\dfrac{m_4}{m_2}k_1 + \dfrac{m_1 + m_4}{m_2}k_3 - \dfrac{m_1 m_4}{m_2}\omega^2\right)k_2 \cos\psi_2}{\Delta}\hat{\chi}_{3n}, \tag{41}$$

$$\hat{\chi}_{4n} = \frac{-\left(\dfrac{m_1}{m_2}k_2 - k_3\right)k_1\cos\psi_1 - \left[\left(1+\dfrac{m_1}{m_2}\right)k_1 + k_3 - m_1\omega^2\right]k_2\cos\psi_2}{\Delta}\hat{\chi}_{3n}, \quad (42)$$

where

$$\Delta = \left[\left(1+\frac{m_1}{m_2}\right)k_1 + k_3 - m_1\omega^2\right]\left[\left(1+\frac{m_4}{m_2}\right)k_2 + k_3 - m_4\omega^2\right] - \left(\frac{m_1}{m_2}k_2 - k_3\right)\left(\frac{m_4}{m_2}k_1 - k_3\right). \quad (43)$$

To capture the coupling between the transverse belt motion and the tensioner arm rotation, general solutions for the transverse response of the belt spans must be obtained. The solution form used here is the one presented by Sack [17]. For belt span 1, the eigenfunction $\phi_{1n}(x)$ can be expressed as

$$\phi_{1n}(x) = \mathrm{e}^{i\omega x/c'_a}[a_1\sin(\omega x/c'_1) + b_1\cos(\omega x/c'_1)], \quad (44)$$

where the effective wave velocity c'_1, the propagation speed c_1 of the transverse wave, and the phase propagation velocity c'_a for span 1 are defined as

$$c'_1 = \frac{c_1^2 - c^2}{c_1}, \quad c_1 = \sqrt{\frac{P_{o1}}{m}}, \quad c'_a = \frac{c_1^2 - c^2}{c}. \quad (45)$$

Using boundary conditions $\phi_{1n}(0) = 0$ and $\phi_{1n}(l_1) = \hat{\chi}_{3n}\sin\psi_1$ to determine the integration constants in the eigenfunction expression (44) leads to

$$a_1 = \frac{\mathrm{e}^{-i\omega l_1/c'_a}\sin\psi_1}{\sin(\omega l_1/c'_1)}\hat{\chi}_{3n}, \quad b_1 = 0. \quad (46)$$

Similarly, for span 2, the eigenfunction can be expressed as

$$\phi_{2n}(x) = \mathrm{e}^{i\omega x/c'_b}[a_2\sin(\omega x/c'_2) + b_2\cos(\omega x/c'_2)], \quad (47)$$

where the effective wave velocity c'_2, the propagation speed c_2 of transverse wave, and the phase propagation velocity c'_b for span 2 are defined as

$$c'_b = \frac{c_2^2 - c^2}{c}, \quad c'_2 = \frac{c_2^2 - c^2}{c_2}, \quad c_2 = \sqrt{\frac{P_{o2}}{m}}. \quad (48)$$

Applying the boundary condition that $\phi_{2n}(0) = \hat{\chi}_{3n}\sin\psi_2$ and $\phi_{2n}(l_2) = 0$, the integration constants in equation (47) can be obtained:

$$a_2 = -\sin\psi_2 \cot(\omega l_2/c_2')\hat{\chi}_{3n}, \quad b_2 = \sin\psi_2 \hat{\chi}_{3n}. \tag{49}$$

Substituting equations (40)–(42), (44) and (47) into the equation of motion for the tensioner arm, equation (13), yields the characteristic equation for eigenvalues of the system

$$\begin{aligned} &P_{t1}\sin^2\psi_1 \cot(\omega l_1/c_1')\omega/c_1' + P_{t2}\sin^2\psi_2\cot(\omega l_2/c_2')\omega/c_2' + k_1\cos^2\psi_1 \\ &\quad + k_2\cos^2\psi_2 + k_4 - m_3\omega^2 \\ &\quad + \frac{(k_1\cos\psi_1 - k_2\cos\psi_2)^2\left(-\dfrac{m_1+m_2+m_4}{m_2}k_3 + \dfrac{m_1 m_4}{m_2}\omega^2\right)}{\Delta} \\ &\quad + \frac{k_1^2\cos^2\psi_1\left(-\dfrac{m_1+m_2+m_4}{m_2}k_2 + m_4\omega^2\right) + k_2^2\cos^2\psi_2\left(-\dfrac{m_1+m_2+m_4}{m_2}k_1 + m_1\omega^2\right)}{\Delta} = 0. \end{aligned} \tag{50}$$

From this equation, it is not difficult to study the effect of different parameters on eigenvalues of the system. For the rotationally dominant modes, since the first two terms on the left side of the characteristic equations are much smaller than the remaining terms, the natural frequencies are mainly determined by the axial stiffness, masses and tensioner arm orientation. Therefore, the natural frequencies should be weak functions of the translating speed. For transversely dominant modes, since $\cot(\omega l_1/c_1')$ or $\cot(\omega l_2/c_2')$ is very large, the natural frequencies are mainly determined by the span tension and the translating speed. Thus, the natural frequencies are expected to decrease significantly with the speed. For the lower order transversely dominant modes, the axial stiffness, masses and tensioner arm orientation have some effect on the natural frequencies while for the higher order modes, the natural frequencies are almost independent on masses of the discrete components and the tensioner arm orientation.

The characteristic equation (50) is a non-linear equation which can be solved numerically. The approach proposed for the analysis of the three-pulley system is readily extended to more complex belt drive systems involving multiple accessories.

After having eigenvalues of the system, the corresponding eigenfunctions can be obtained by substituting these eigenvalues into equations (40)–(42), (44) and (47). It is noted that both the amplitudes and the shapes of the complex eigenfunctions of the belt spans and the amplitudes of the real eigenvectors of the discrete components depend on the normalization.

4. RESPONSE TO ARBITRARY EXCITATION

The response of a single belt subjected to general excitations and initial conditions was obtained by Wickert and Mote [3]. In this study, the modal analysis method for a single belt is extended to the hybrid subsystem 2 while the response of subsystem 1 can be directly calculated using the results given in reference [3].

Consider the expansion

$$\mathbf{U} = \sum_{n=1}^{\infty} \xi_n^R \boldsymbol{\psi}_n^R + \xi_n^I \boldsymbol{\psi}_n^I \tag{51}$$

as the solution of equation (25). The components $\xi_n^R(t)$ and $\xi_n^I(t)$ of the generalized co-ordinates are real, and it is assumed that the expansion is complete. Substituting equation (51) into (25), forming an inner product with $(\boldsymbol{\psi}_n^R \quad \boldsymbol{\psi}_n^1)$ and using the orthonormality conditions leads to the following equations of motion for modal co-ordinates:

$$\xi_n^R - \omega_n \xi_n^I = q_n^R(t), \quad \xi_n^I + \omega_n \xi_n^R = q_n^I(t), \tag{52}$$

where

$$q_n^R(t) = -\omega_n \int_0^{l_1} \phi_{1n}^I f_1(x, t)\, \mathrm{d}x - \omega_n \int_0^{l_2} \phi_{2n}^I f_2(x, t)\, \mathrm{d}x, \tag{53}$$

$$q_n^I(t) = \omega_n \int_0^{l_1} \phi_{1n}^R f_1(x, t)\, \mathrm{d}x + \omega_n \int^{l_2} 2_0 \phi_{2n}^R f_2(x, t)\, \mathrm{d}x$$
$$+ \omega_n \hat{\chi}_{1n} f_3(t) + \omega_n \hat{\chi}_{2n} f_4(t) + \omega_n \hat{\chi}_{3n} f_5(t) + \omega_n \hat{\chi}_{4n} f_6(t). \tag{54}$$

The solutions of equation (52) are given as

$$\xi_n^R(t) = \int_0^t [q_n^R s) \cos(\omega_n (t-s)) + q_n^I(s) \sin(\omega_n (t-s))]\, \mathrm{d}s$$
$$+ \xi_n^R(0) \cos(\omega_n t) + \xi_n^I(0) \sin(\omega_n t), \tag{55}$$

$$\xi_n^t(t) = \int_0^t [q_n^t s) \cos(\omega_n (t-s)) - q_n^R(s) \sin(\omega_n (t-s))]\, \mathrm{d}s$$
$$+ \xi_n^I(0) \cos(\omega_n t) - \xi_n^R(0) \sin(\omega_n t), \tag{56}$$

where the initial values of the modal co-ordinates are

$$\xi_n^R(0) = \langle \mathbf{AU}_0, \boldsymbol{\Psi}_n^R \rangle, \quad \xi_n^I(0) = \langle \mathbf{AU}_0, \boldsymbol{\Psi}_n^I \rangle. \tag{57}$$

Following equation (51), the field variable expansion becomes

$$\mathbf{W} = \sum_{n=1}^{\infty} \xi_n^R \phi_n^R + \xi_n^I \phi_n^I. \tag{58}$$

5. STEADY STATE RESPONSE SUBJECTED TO HARMONIC EXCITATION

In the previous section, the response of serpentine belt drive systems to arbitrary excitation is obtained using the eigenfunction expansion method. This result is obviously applicable to the steady state response of the system subjected to non-resonance harmonic excitations. However, since the expression is in terms of the linear mode shapes, it would be very difficult to use in the direct perturbation analysis for non-linear systems. An explicit exact expression for the steady state response is still preferred.

Assume that the harmonic excitations are in the form

$$\mathbf{F} = \{f_1(x, t) f_2(x, t) f_3(x, t) f_4(x, t) f_5(x, t) f_6(x, t)\}^T \mathrm{e}^{i\omega t}, \tag{59}$$

where ω is the excitation frequency. The steady state response of the system is also harmonic with the same oscillation frequency,

$$\mathbf{W} = \{\Phi_1(x) \Phi_2(x) \tilde{\chi}_1 \tilde{\chi}_2 \tilde{\chi}_3 \tilde{\chi}_4\}^T \mathrm{e}^{i\omega t}. \tag{60}$$

Substituting equations (59) and (60) into the equation of motion of belt span 1 and eliminating $\mathrm{e}^{i\omega t}$ yields the two-point boundary-value problem

$$-m\omega^2 \Phi_1(x) + 2i\omega mc \frac{\mathrm{d}\Phi_1(x)}{\mathrm{d}x} - P_{t1} \frac{\mathrm{d}^2\Phi_1(x)}{\mathrm{d}x^2} = f_1(x), \tag{61}$$

$$\Phi_1(0) = 0, \quad \Phi_1(l_1) = \tilde{\chi}_3 \sin\psi_1. \tag{62}$$

The general solution of equation (61) is

$$\Phi_1(x) = \mathrm{e}^{i\omega x/c'_a}[a_1 \sin(\omega x/c'_1) + b_1 \cos(\omega x/c'_1)] + \hat{\Phi}_1(x), \tag{63}$$

where $\hat{\Phi}_1(x)$ is the particular solution of equation (61). Applying boundary conditions (62), the integration constants in equation (63) can be obtained as

$$a_1 = \frac{[\tilde{\chi}_3 \sin\psi_1 - \hat{\Phi}_1(l_1)]\, \mathrm{e}^{-i\omega l_1/c'_a} + \hat{\Phi}_1(0)\cos(\omega l_1/c'_1)}{\sin(\omega l_1/c'_1)}, \quad b_1 = -\hat{\Phi}_1(0). \tag{64}$$

Similarly, for span 2, the spatial dependence function is given as

$$\Phi_2(x) = \mathrm{e}^{i\omega x/c'_b}[a_2 \sin(\omega x/c'_2) + b_2 \cos(\omega x/c'_2)] + \hat{\Phi}_2(x), \tag{65}$$

with boundary conditions

$$\Phi_2(0) = \tilde{\chi}_3 \sin\psi_2, \quad \Phi_2(l_2) = 0, \tag{66}$$

where $\hat{\Phi}_2(x)$ is the particular solution. The integration constants a_2 and b_2 are obtained by using the boundary conditions

$$a_2 = \frac{-\hat{\Phi}_2(l_2)\,\mathrm{e}^{-i\omega l_2/c'_b}}{\sin(\omega l_2/c'_2)} - (\tilde{\chi}_3 \sin\psi_2 - \hat{\Phi}_2(0))\cot(\omega l_2/c'_2), \quad b_2 = \tilde{\chi}_3 \sin\psi_2 - \hat{\Phi}_2(0). \tag{67}$$

Using equations (63) and (65) for the belt response in the equation of motion for the tensioner arm, the terms in equation (13) involving w_1 and w_2 can be simplified as

$$-P_{t1} w_{1,x}|_{l_1} + mcw_{1,t}|_{l_1} = \left(-P_{t1}\sin\psi_1 \cot(\omega l_1/c'_1)\frac{\omega}{c'_1}\tilde{\chi}_3 + f_7\right)\mathrm{e}^{i\omega t}, \tag{68}$$

$$-P_{t2} w_{2,x}|_0 + mcw_{2,t}|_0 = \left(P_{t2}\sin\psi_2 \cot(\omega l_2/c'_2)\frac{\omega}{c'_2}\tilde{\chi}_3 + f_8\right)\mathrm{e}^{i\omega t}, \tag{69}$$

where

$$f_7 = -\frac{P_{t1}\omega\,\mathrm{e}^{i\omega l_1/c'_a}\hat{\Phi}_1(0)}{c'_1\sin(\omega l_1/c'_1)} + \left(i\omega mc + P_{t1}\cot(\omega l_1/c'_1)\frac{\omega}{c'_1}\right)\hat{\Phi}_1(l_1) - P_{t1}\hat{\Phi}'_1(l_1), \tag{70}$$

$$f_8 = \frac{P_{t2}\omega\,\mathrm{e}^{-i\omega l_2/c'_b}\hat{\Phi}_2(l_2)}{c'_2\sin(\omega l_2/c'_2)} + \left(i\omega mc - P_{t2}\cot(\omega l_2/c'_2)\frac{\omega}{c'_2}\right)\hat{\Phi}_2(0) - P_{t2}\hat{\Phi}'_2(0). \tag{71}$$

Inserting equations (68) and (69) into the equation of motion of the tensioner arm, rewriting the resulting equation and the three equations of motion for the pulleys into matrix form, and eliminating $\mathrm{e}^{i\omega t}$ leads to the algebraic equation

$$(\mathbf{K}_{DD} - \mathbf{M}_{DD}\omega^2)\begin{Bmatrix}\tilde{\chi}_1\\ \tilde{\chi}_2\\ \tilde{\chi}_3\\ \tilde{\chi}_4\end{Bmatrix} = \begin{Bmatrix} f_3\\ f_4\\ f_5 + f_7\sin\psi_1 - f_8\sin\psi_2\\ f_6\end{Bmatrix}, \tag{72}$$

where

$$\mathbf{K}_{DD} = \begin{bmatrix} k_1 + k_3 & -k_1 & -k_1\cos\psi_1 & -k_3\\ -k_1 & k_1 + k_2 & k_1\cos\psi_1 - k_2\cos\psi_2 & -k_2\\ -k_1\cos\psi_1 & k_1\cos\psi_1 - k_2\cos\psi_2 & k_{33} & k_2\cos\psi_2\\ -k_3 & -k_2 & k_2\cos\psi_2 & k_2 + k_3\end{bmatrix}, \tag{73}$$

$$k_{33} = k_1\cos^2\psi_1 + k_2\cos^2\psi_2 + k_4 + P_{t1}\sin^2\psi_1\cot(\omega l_1/c'_1)\frac{\omega}{c'_1} + P_{t2}\sin^2\psi_2\cot(\omega l_2/c'_2)\frac{\omega}{c'_2}, \tag{74}$$

$$\mathbf{M}_{DD} = \begin{bmatrix} m_1 & 0 & 0 & 0 \\ 0 & m_2 & 0 & 0 \\ 0 & 0 & m_3 & 0 \\ 0 & 0 & 0 & m_4 \end{bmatrix}. \tag{75}$$

Substituting the solution of equation (72) into equations (63) and (65), the explicit exact expression for the response of the serpentine belt drive system is derived. It is noted that the solution procedure does not involve eigenfunction expansion. The solution in this form is very convenient to be used in the direct perturbation analysis of the corresponding non-linear problem.

6. NUMERICAL RESULTS

In this section, numerical results of natural frequencies and the linear forced vibration response of serpentine belt drive systems are presented. Effects of the transport speed and the tensioner arm orientation on natural frequencies are discussed.

Two prototypical systems simulated are identical to those proposed by Beikmann *et al*. [13] where natural frequencies of the two systems were calculated using the iteration approach. In this study, natural frequencies are obtained directly from the characteristic equation and the response is calculated from the exact closed-form expressions. The physical properties are shown in Table 1. The baseline system has a first rotationally dominant mode frequency nearly twice that of the first transverse mode of span 3. The modified system is identical to the first, except for the addition of a 0·0758-kg mass to the tensioner arm.

A comparison of natural frequencies among those obtained from experiment [13], Holzer's method [13] and the approach proposed in the paper is shown in Tables 2 and 3. It can be seen that correlation among the three methods is quite good. The first mode, for both systems, is dominated by span 3 vibration. Since there is no coupling between the transverse vibration of span 3 and pulley rotations, the change of properties of subsystem 2 does not alter the natural

TABLE 1

The physical properties for the prototypical systems

	Pulley 1	Pulley 2	Tensioner arm	Pulley 4
Spin axis co-ordinates	(0·5525, 0·0556)	(0·3477; 0·05715)	(0·2508, 0·0635)	(0·0, 0·0)
Radii (m)	0·0889	0·0452	0·097	0·02697
Rotational inertia (kg-m^2)	0·07248	0·00293	0·001165	0·000293
Other physical properties	Belt modulus: EA = 170 000 N, m = 0·1029 kg/m, Tensioner spring constant: k_r = 54·37 N-m/rad, Tensioner pulley mass: 0·302 kg (baseline), 0·378 kg (modified)			

TABLE 2

Comparison of the natural frequency of the baseline system at zero speed

Mode No.	Experimental (Hz)	Holzer's method (Hz)	Characteristic equation (Hz)	Dominant mode
1	33·0	32·03	32·03	1st mode, span 3
2	51·75	50·52	50·53	1st mode, span 2
3	62·5	62·22	62·18	1st rotational
4	N/A	N/A	102·50	2nd mode, span 2
5	N/A	N/A	114·19	1st mode, span 1
6	N/A	N/A	153·75	3rd mode, span 2
7	N/A	N/A	218·51	2nd mode, rotational

frequency of span 3. This is demonstrated by the negligible difference in the fundamental natural frequency of span 3 between the baseline and modified systems. The second mode is the vibration dominated by span 2. It has a frequency of 50·53 Hz in the baseline system and 50·27 Hz in the modified system. The vibration mode of the baseline system is shown in Figure 2. The third mode is dominated by the tensioner arm rotation. It has a natural frequency of 62·18 Hz in the baseline system and 58·27 Hz in the modified system. This demonstrates the significant effect of the mass on the natural frequency of this mode. As predicated in the modal analysis, there is a significant coupling between the span's transverse vibration and the tensioner arm rotational vibration, as shown in Figure 3.

The effect of the tensioner arm orientation on natural frequencies is shown in Table 4. It can be seen that the tensioner arm orientation has a significant effect on the rotationally dominant mode while it has less effect on the transversely dominant mode for zero speed. From the characteristic equation, it is seen that the tensioner arm orientation affects the effective tensioner stiffness and the coupling between the tensioner arm and the transverse span motion. Therefore, the tensioner arm orientation influences rotationally dominant modes significantly. With the increase of the translating speed, the tensioner arm

TABLE 3

Comparison of the natural frequency of the modified system at zero speed

Mode No.	Experimental (Hz)	Holzer's method (Hz)	Characteristic equation (Hz)	Dominant mode
1	33·0	32·03	32·03	1st mode, span 3
2	51·5	50·52	50·27	1st mode, span 2
3	58·0	58·81	58·57	1st rotational
4	N/A	N/A	102·50	2nd mode, span 2
5	N/A	N/A	114·19	1st mode, span 1
6	N/A	N/A	153·75	3rd mode, span 2
7	N/A	N/A	203·19	2nd mode, rotational

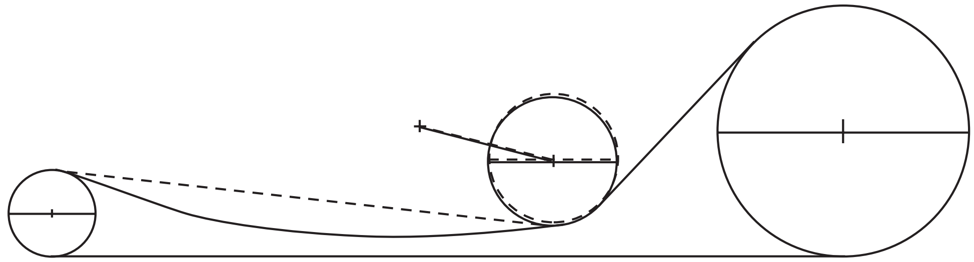

Figure 2. Span 2 transversely dominant vibration mode of the baseline system: —, the baseline sytem; ······, mode shape.

orientation will change the span tensions and thus will significantly affect the natural frequency of transversely dominant modes.

The effect of the translating speed on the natural frequencies of the single moving belt has been studied extensively [7, 8, 11]. However, for the whole serpentine drive system where the coupling between pulleys and belt spans exists, this effect needs further consideration. Beikmann *et al*. [13] investigated this effect using experimental and numerical methods. In this paper, the relations between the translating speed and natural frequencies are obtained directly from the characteristic equation, as shown in section 3. Figures 4 and 5 illustrate the relation between natural frequencies and the engine speed for the baseline system and the modified system, respectively. Higher order transversely dominant mode frequencies are not shown in Figures 4 and 5 since they are simply integer times the first transversely dominant mode frequency of span 1 or span 2. It is evident that the natural frequencies of rotationally dominant modes remain nearly constant while those of transversely dominant modes decrease with the speed. These results agree very well with the conclusions by Beikmann *et al*. [13]. It is noted that there are some irregularities for the second rotationally dominant mode. This is because at some operating speeds, the frequency of a higher order transversely dominant mode not shown in Figures 4 and 5 approaches that of the second rotationally dominant mode. This phenomenon is termed "curve veering" which indicates large and complementary changes in the associated modes. From the characteristic equation (50), it can be seen that one of the first two terms on the left side of equation (50) becomes more significant at curve veering, resulting in some irregularities at some speeds.

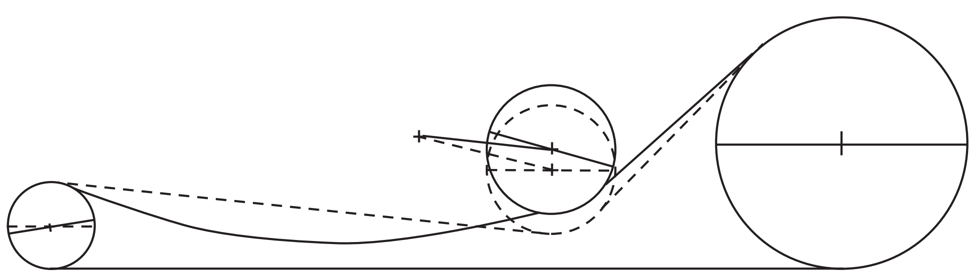

Figure 3. Tensioner arm rotationally dominant vibration mode of the baseline system: —, the baseline system; ······, mode shape.

TABLE 4

Effect of the tensioner arm orientation on the natural frequency (Hz) of the baseline system at zero speed

Mode No.	(ψ_1, ψ_2)			
	(45·78°, 91·26°)	(49·54°, 87·51°)	(53·29°, 83·76°)	(60·79°, 76·26°)
1	32·03	32·03	32·03	32·03
2	50·53	50·63	50·70	50·80
3	62·18	63·81	65·25	67·43
4	102·50	102·50	102·50	102·5-
5	114·19	114·19	114·19	114·19
6	153·75	153·75	153·75	153·75
7	218·51	219·54	219·41	219·67

The steady state response of the serpentine belt system subjected to a harmonic excitation is shown in Figures 6 to 8. The excitation is imposed on pulley 4 with the amplitude of excitation 2·697 N-m and the excitation frequency 124·36 Hz. Figures 6 and 7 show 3-D diagrams for the response of spans 1 and 2 with respect to time t and space x and Figure 8 shows the response of discrete

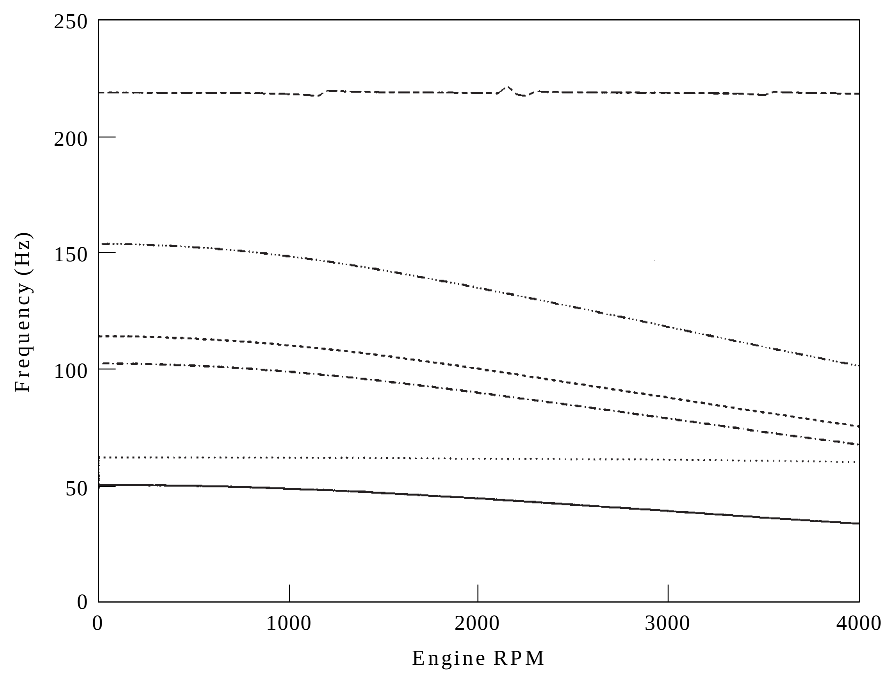

Figure 4. Natural frequencies of the baseline system: —, mode 1; ······, mode 2; -·- , mode 3; - - -, mode 4; -·-·-·-·, mode 5; – – –, mode 6.

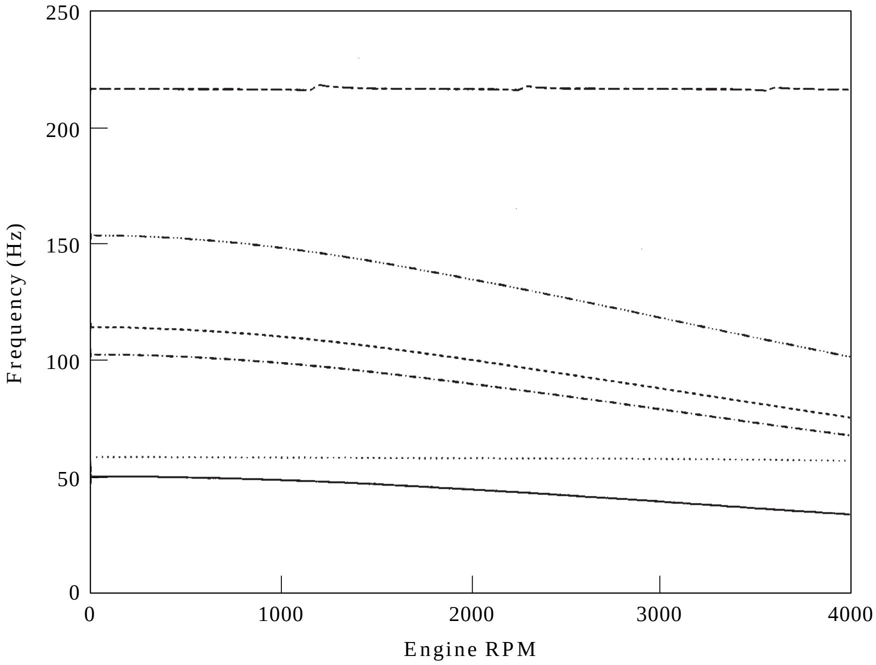

Figure 5. Natural frequencies of the modified system: —, mode 1; ······, mode 2; -·-, mode 3; ---, mode 4; -···-··, mode 5; –––, mode 6.

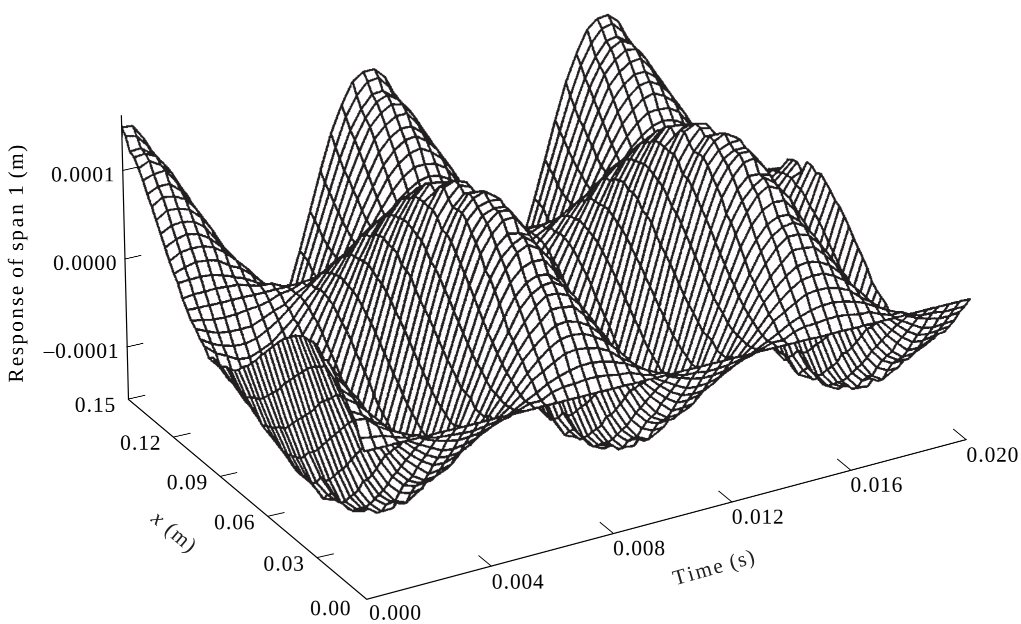

Figure 6. The steady state response of span 1.

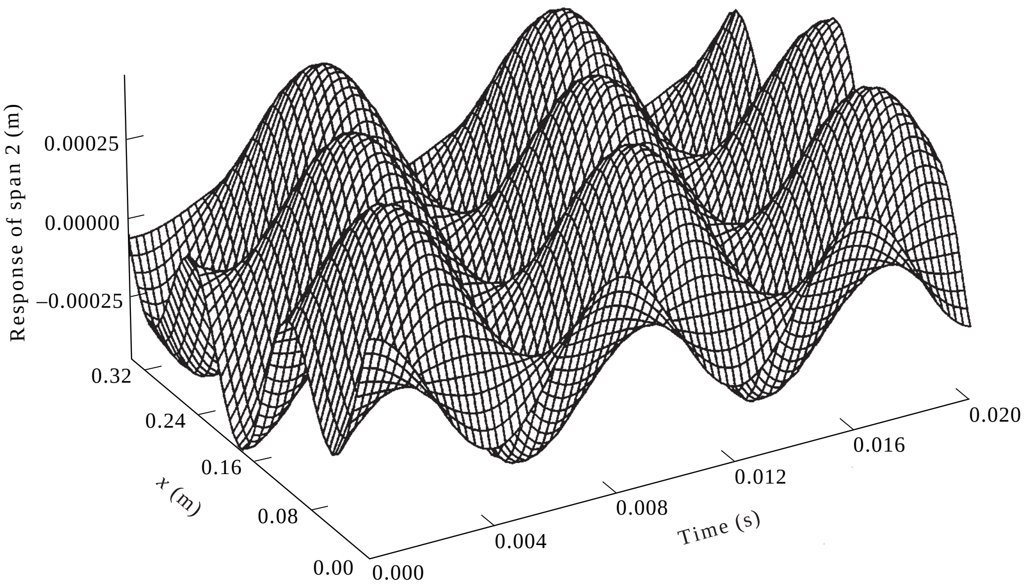

Figure 7. The steady state response of span 2.

components. It is seen that the response of span 1 at $x = 0$ is zero while it is not equal to zero at the other end due to the coupling with the tensioner arm. The response of span 2 at $x = 0$ is not equal to zero. The response of the tensioner arm is the biggest compared with that of other pulleys. It is noted that for the linear model, when the excitation frequency is not equal to the natural frequency of the system, the dynamic response is very small. However, for the non-linear model, under the condition of the internal resonance, the response may be very

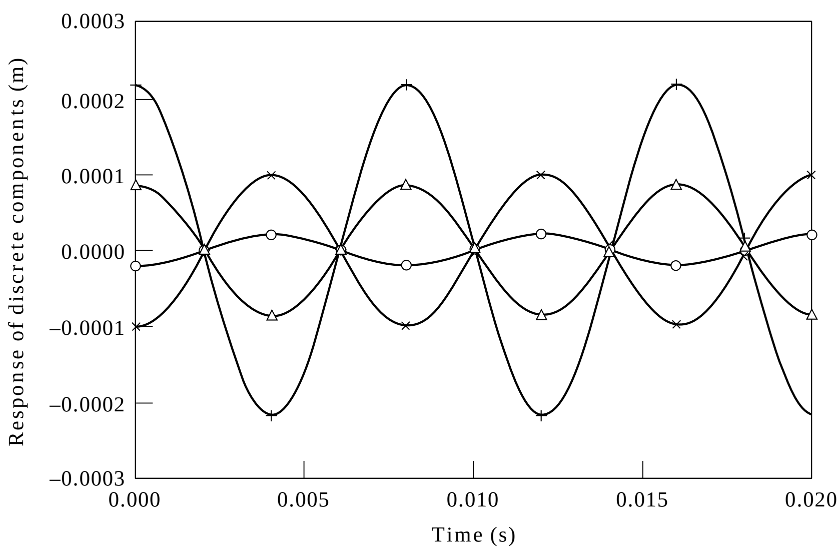

Figure 8. The steady state response of discrete components: ○, pulley 1; +, pulley 2; ×, tensioner arm; △, pulley 4.

large.

7. CONCLUSION

The modal analysis of the linear prototypical serpentine belt drive system is performed in this study. The entire system is divided into two subsystems: subsystem 1 with belt span 3 only and subsystem 2 with other components. In the linear analysis, the equations of motion of these two subsystems are uncoupled. Therefore, it is convenient to deal with these two systems separately.

Although the eigenvalues and eigenfunctions of the prototypical system were calculated in a previous study [13], it is not convenient to investigate the effects of different parameters on eigenvalues since an iteration approach is employed in reference [13]. In this paper, the explicit exact characteristic equation for eigenvalues is derived without using the iteration approach. From the characteristic equation (50), the following two conclusions about the effect of the design parameters on natural frequencies can be drawn:

- The translating speed has a significant effect on natural frequencies of transversely dominant modes while it has less effect on those of rotationally dominant modes. The natural frequencies of transversely dominant modes decrease with the increase of translating speed.
- The tensioner arm orientation influences natural frequencies of rotationally dominant modes greatly. At lower translating speed, the effect of the tensioner arm on transversely dominant modes is small. With the increase of the translating speed, this effect also increases.

The response of the serpentine belt drive system subjected to arbitrary excitations is represented as a superposition of orthogonal eigenfunctions. When the excitations are non-resonance harmonic, the explicit exact solution without using eigenfunction expansion is derived. This kind of expression is particularly useful in the direct perturbation analysis of the corresponding non-linear problems.

ACKNOWLEDGMENT

This research is financially supported by a research grant from the National Science and Engineering Research Council of Canada.

REFERENCES

1. R. SKUTCH 1897 *Annals of Physics and Chemistry* **61**, 190–195. Über die Bewegung eines gespannten Fadens.
2. F. R. ARCHIBALD and A. G. EMSLIE 1958 *ASME Journal of Applied Mechanics* **25**, 347–348. The vibration of a string having a uniform motion along its length.
3. J. A. WICKERT and C. D. MOTE, JR. 1990 *ASME Journal of Applied Mechanics* **57**, 738–744. Classical vibration analysis of axially moving continua.
4. C. D. MOTE, JR. 1966 *ASME Journal of Applied Mechanics* **33**, 463–464. On the non-linear oscillation of an axially moving string.

5. A. L. Thurman and C. D. Mote, Jr. 1969 *ASME Journal of Applied Mechanics* **36**, 83–91. Free, periodic, non-linear oscillation of an axially moving strip.
6. V. A. Bapat and P. Srinivasan 1967 *ASME Journal of Applied Mechanics* **34**, 775–777. Non-linear transverse oscillation in traveling strings by the method of harmonic balance.
7. J. Moon and J. A. Wickert 1997 *Journal of Sound and Vibration* **200**, 419–431. Non-linear vibration of power transmission belts.
8. L. E. Hawker 1991 *Ph.D. Dissertation*, *University of Windsor*, *Ontario*, *Canada*. A vibration analysis of automotive serpentine accessory drive systems.
9. C. R. Barker, L. R. Oliver and W. F. Breig 1991 *SAE Paper* 910687. Dynamic analysis of belt drive tension forces during rapid engine acceleration.
10. S. J. Hwang, N. C. Perkins, A. G. Ulsoy and R. J. Meckstroth 1994 *ASME Journal of Vibration and Acoustics* **116**, 71–78. Rotational response and slip prediction of serpentine belt drive systems.
11. T. C. Kraver, G. W. Fan and J. J. Shah 1996 *ASME Journal of Mechanical Design* **118**, 306–311. Complex modal analysis of a flat belt pulley system with belt damping and Coulomb-damped tensioner.
12. A. G. Ulsoy, J. E. Whitsel and M. D. Hooven 1985 *ASME Journal of Vibrations*, *Acoustics Stress*, *and Reliability in Design* **107**, 282–290. Design of belt-tensioner systems for dynamic stability.
13. R. S. Beikmann, N. C. Perkins and A. G. Ulsoy 1996 *ASME Journal of Vibration and Acoustics* **118**, 406–413. Free vibration of serpentine belt drive systems.
14. R. S. Beikmann, N. C. Perkins and A. G. Ulsoy 1996 *ASME Journal of Vibration and Acoustics* **118**, 567–574. Nonlinear coupled vibration response of serpentine belt drive systems.
15. L. Meirovitch 1974 *AIAA Journal* **12**, 1337–1342. A new method of solution of the eigenvalue problem for gyroscopic systems.
16. L. Meirovitch 1975 *ASME Journal of Applied Mechanics* **42**, 446–450. A modal analysis for the response of linear gyroscopic systems.
17. R. A. Sack 1954 *British Journal of Applied Physics* **5**, 224–226. Transverse oscillations in travelling strings.